Title

Molecular dynamics simulations of single grain pure aluminum in a vice fixture for nanomanufacturing applications

Authors

Garcia, Destiny R
Zhang, Zhibo
Linke, Barbara S
et al.

Publication Date

2018-11-01

DOI

10.1016/j.cirpj.2018.07.005

Peer reviewed

Molecular Dynamics Simulations of Single Grain Pure Aluminum in a Vice Fixture for Nanomanufacturing Applications

Destiny R. Garcia[1], Zhibo Zhang[2], Barbara S. Linke[1*], Herbert M. Urbassek[2]

[1]University of California Davis, Mechanical and Aerospace Engineering Department
1 Shields Ave, Davis, CA 95616
USA

[2]Physics Department and Research Center OPTIMAS
University Kaiserslautern,
Erwin-Schrödinger-Straße
67663 Kaiserslautern
Germany

*Corresponding author
Email: bslinke@ucdavis.edu

Keywords

Machining Distortions, Machining Deformations, Materials Science, Residual Stresses, Nano-scale manufacturing, Micro-scale Manufacturing, Work-holding devices, Fixtures

Abstract

Although nano and macro manufacturing encompass two different scales of machining, investigating both is essential for understanding machining distortions and deformations. In both macro and nano fabrication, the fixture is the primary means of securing the workpiece in place while performing the manufacturing operations. Understanding the fixture design is a critical aspect relating the two different scales of manufacturing.

This paper describes a method involving atomistic simulation for understanding machining distortions for the macro scale by investigation of nano machining and work holding devices.

This research aims to help bridge the knowledge gap in manufacturing of macro and nano scale applications. The simulations performed showed that the fixture influences the machining distortions and the critical stress concentrations on the workpiece.

1. INTRODUCTION

Current research states that mechanical cutting processes are very important in bridging the gap of macro and nano domains for manufacturing functional components [1]. As the advancements of nano-machining stride forward, understanding the machining distortions and deformations related to the nano-scale becomes a vital part of mastering this field. In order to investigate machining distortions, understanding fixture design is a critical aspect.

Machining distortions in the macro setting of manufacturing are defined as the deviation of a part change after being released from a fixture [2]. These distortions are not caused by dimensional inaccuracies, machining intolerances, or over and under machining [2]. Machining distortions result in a significant economic loss due to reworking, remanufacturing and/or rejecting components that do not meet specifications. This study will investigate distortion at the nanoscale using molecular dynamics simulations to bridge the gap between nano and macro machining. The next chapter will investigate the state of the art of machining distortion and residual stresses, as well as nano machining and fixtures. The following sections will include a methods section, results and discussion, and a conclusion.

2. BACKGROUND: STATE OF THE ART

2.1 Machining Distortion

Residual stresses, or the stresses locked into the workpiece, are a primary factor contributing to machining distortions. The residual stresses are induced by prior material processing steps such as rolling, forging, heat-treatment, etc. – which are needed in the specific industries for high strength and other desirable material properties. The evolution of the microstructural deformation during the forming process causes residual stresses, which affect the mechanical properties and durability [3].

With such efforts to understand residual stresses, capabilities for prediction and simulations of machining distortion are being developed. Current industrial solutions to machining distortion involve machining incrementally in small symmetrical steps until the part is within tolerance and desired dimensions [4]. However, this practice is slow and costly, and is intolerant to variations in the bulk residual stress state of inbound material. Using advanced FEM/FEA software, prediction tools have been developed to minimize machining distortion [5]. Recent FEM advancements for machining distortion include: simplifying distortion to a bending moment, which is a function of the residual stress profile [6 - 8]; using element "birth and death" to simulate material removal and deformations [9]; modeling residual stresses used in milling experiments using relaxation techniques [10]; and modeling quenched material to simulate machining deformations related to materials processing [11].

Further understanding and new knowledge about part distortion is critical for the industry to advance and minimize or control distortion. Recent advancements in distortion engineering have led to a design against distortion approach in which engineers attempt to be proactive to prevent costly deformations [2]. In-process deformation measurements of thin-walled workpieces have also been explored to understand deformations while manufacturing [12].

After obtaining residual stress profiles of the workpiece cross-section, machinists and technicians can create an optimized workflow to help minimize distortion [2]. Machining strategies have been investigated such that the material removal steps are able to minimize part distortion based on geometrical symmetries [6]. Analysis of all the production steps in the manufacturing of mechanical gears has been studied to minimize shape deviations [13]. Although some of the presented models are suitable in predicting distortion at the macro-scale, there is a gap in the research to understand machining distortions in nano-manufacturing.

2.2 Nano-Machining

Manufacturing at the micro and nano-scales are increasingly in high demand for multiple industries such as electronics, bio-medical engineering, aerospace, etc. The motivation to create smaller devices stems from the need to manufacture workpieces with better performance, less materials, higher efficiencies and being less expensive [14]. Nanofabrication techniques include photolithography, chemical etching, laser machining, atomic force lithography, and focused ion beam lithography [15].

Manufacturing at the nano-scale includes work areas related to the atomic and material sciences. Such applications in manufacturing have an accuracy of high precision and ultra-precision [1]. As the manufacturing scale decreases, challenges arise in accuracy, surface quality, and integrity of the machined part. Such challenges can emerge from tool edge geometry, grain size, and grain orientation [14], even though these factors have little or no effect on the macro-scale. Critical issues associated with understanding the differences

between macro and micro/nano machining include the miniaturization of components, tools, and manufacturing processes [1].

Advancements in the nano-manufacturing research include nano-mechanical machining to make complex shapes by plowing techniques of semiconductor structures [16]. Molecular dynamics simulations of nanometric cutting mechanisms of amorphous alloys were investigated to study the effects of nano machining [17]. Atomic scale deformations in silicon mono-crystals were studied using molecular dynamics under two and three body contact sliding [18]. Molecular dynamic simulations on monocrystalline copper revealed groove forming characteristics and mechanisms in nano-milling [15].

Other developments include understanding the relationship between the cutting force and tool wear for micro machining [19]. Estimations of the tool wear for micro-machining were studied using a periodic tool inspector [19]. Many of the researchers who study micro and nano machining use the cutting force to improve the overall quality [1]. At these small scales, the dynamics of the tool and workpiece differ from those at the macro scale. Current research shows there is a lack in the knowledge pertaining to machining distortion at the nano-scale and its relation to macro machining distortions.

2.3 Machining Fixtures

To initially understand the relation of machining distortions to both macro and nano-manufacturing, the fixture or work-holding device is an important feature to investigate. In both macro and nano fabrication, the fixture is the primary means of securing the workpiece in place while performing the manufacturing operations.

The primary tasks of the fixture during machining is to: define the position and orientation of the workpiece in the machine tool, maintain defined workpiece location throughout machining forces, and to guide the machining forces of the machine structure [20-22]. During machining, the workpiece experiences minor deformations due to the clamping forces. Fixture layout and clamping forces are two main aspects that influence machining deformation [23]. Contact forces between workpiece and fixture influence the workpiece during machining [24]. The forces acting in the contact region during clamping are important for understanding workpiece deformation [24].

Fixtures can include step clamps, quick release clamps, plain style precision clamps, vice jaw systems, table plate, CNC fixture, etc. [25]. Fixtures are an essential element of the machining system related to both the process and machine tool [22]. Machining distortions directly relate to the fixture as the fixture releases the workpiece and the deformations occur during part re-equilibrations [2].

Advancements in understanding fixture design include computer aided fixture design (CAFD) with respect to information support such as geometry, location, material properties, machining information, applied forces, tolerance requirements, and displacements [26]. Intelligent fixtures for deformation compensation of high performance machining parts have been studied to reduce machining distortions [22]. The optimal clamping forces for multiple clamp fixtures subjected to quasi-static machining forces were determined by Li [27]. FEM was used to control machining deformation through fixture layout design and clamping force optimization [23].

Current approaches for supporting fixture design via CAFD suggest more research in cohesive fixture design support and supporting the detailed design of a fixture's physical structure [28]. Flexible fixture design and automation have been investigated to determine current issues and future directions [29].

FEM combined with contact elasticity models shows that it is possible to calculate contact load and pressure for a frictional workpiece fixture system to further investigate workpiece deformation [24]. Intelligent fixture optimization has been investigated to determine the optimal positions of locating and clamping elements during machining [30-31]. Machining fixtures are an essential scope of machining systems to accurately remove material [22].

This study aims to use molecular dynamics (MD) as a means to study fixtures directly related to machining distortions for nano applications of single grain pure aluminum in a vice fixture for nano-manufacturing applications.

3. METHODS

3.1 Work-Holding Device Model

The work-holding device, or fixture, is a key factor related to machining distortion. The work-holding device is the main means in which the workpiece sits: before, during, and released from, after machining. Machining distortions are caused primarily from the bulk residual internal stresses, but also arise from the clamping stresses and the induced machining stresses.

In the macro setting, machining distortions are primarily caused by the bulk residual stress accounting for almost 90% of the distortion [7]. For this study, it was hypothesized that the clamping stresses are critical for smaller machined parts such as nano and micro machining. The smaller the workpiece, the greater the influence of outside machining parameters such as clamping forces, thermal stresses, workpiece thickness, etc. than compared to larger macro workpieces.

Material removal, which happens while the workpiece is clamped inside the fixture, leads to machining distortions as the workpiece re-equilibrates its internal residual stresses after being unclamped (or released from the fixture). Distortion caused from clamping stresses can only be found from machining distortion clamping simulations due to its minor overall effect in machining distortions.

Carrying out clamping simulations can determine the distortions caused by clamping factors alone. Simulating the workpiece as it is clamped in the fixture will provide knowledge about the importance of clamping mechanisms related to machining distortions.

3.2 Work-Holding Device Simulation

In order to study the effects of a vice fixture with respect to nano-manufacturing of pure Aluminum, a molecular dynamics simulation is conducted with different workpiece shapes mounted in the fixture including: a bar, a U-shape prism and a L-shape prism, using the LAMMPS Molecular Dynamics Simulator [32]. The simulation volume is set up as a box with a size of 80.99 nm x 40.50 nm and 60.74 nm in xyz coordinate axes. The model contains approximately 12,040,000 atoms. The workpiece consists of a single crystal of Al; this material

crystallizes in the face-centered-cubic (FCC) structure with a lattice spacing of 4.032 Å. The crystal <100> axes are aligned with the edges of the workpiece, such that all workpiece surfaces have {100} orientation. The interactions between the Al atoms in this system are described by a potential of the embedded-atom-model (EAM) class originally developed by Daw and Baskes [33]; the actual potential used here for Al [34] has been optimized to describe, among others, elastic properties and defect energetics correctly. The vice is assumed to be of diamond; it is considered rigid in this study. The Al-diamond interaction is modeled by a purely repulsive potential; this potential is obtained from a Lennard–Jones potential by prescribing a cut-off distance equal to 4.2 Å at its minimum and then shifting it such that the energy and force are continuous at the cut-off radius [35].

Before starting the MD simulation, the system is relaxed, such that all components of the stress tensor reach values less than 3 MPa, and the temperature is stabilized at 300K (±1K). Each of the two vices is composed of 239,410 carbon atoms arranged in a rigid diamond lattice structure. The vice structures are represented as plate shapes with a thickness of 1.4 nm and a height of 34 nm. The molecular-dynamics simulations are performed in an isothermal-isobaric (NPT) ensemble during relaxation and in the microcanonical (NVE) ensemble during fixture. As thermostat we employ a velocity-scaling algorithm.

As shown in Figure 1, these two vices clamp the bottom half of aluminum bar while the speed of each vice closing is 10 m/s. This velocity while being too large for fixture applications, has been selected for computational convenience; such a value is standard in molecular dynamics studies of machining applications [36]. The Al bar is fixed when each vice moves into

it by 2 nm. The vice fixture is modeled to have an infinitely long depth in y direction by using periodic boundary conditions.

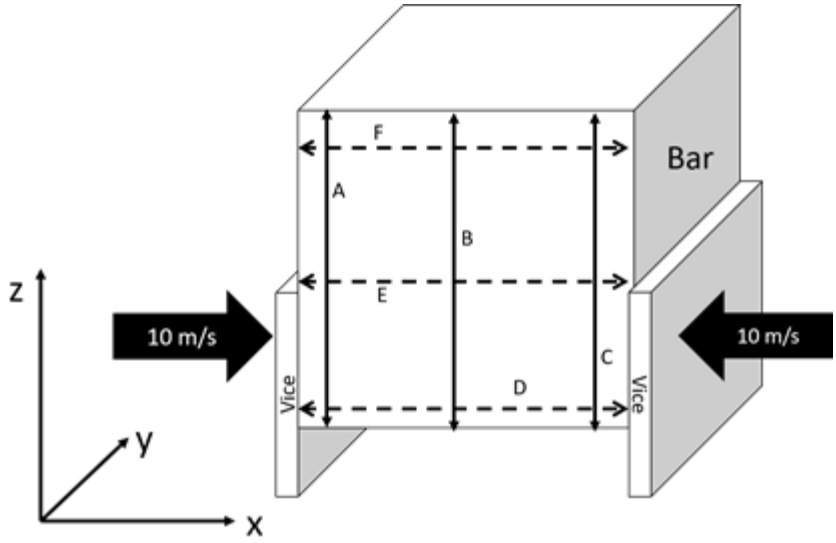

Figure 1. The two vices clamp the bottom half of the aluminum bar. Heights (A, B, C) and lengths (D, E, F) are shown for result references.

The simulation setup is created such that the vice plates hold onto the bottom half of the workpiece, with a closing velocity of 10m/s. The height (solid lines A, B and C) and the length (dashed lines D, E and F) of the workpiece are evaluated as a measure of the distortion. For the U-shape, the referenced height, B is half of the original height. For the L-shape, the reference height, C, and length, F, are half of the original height and length, respectively.

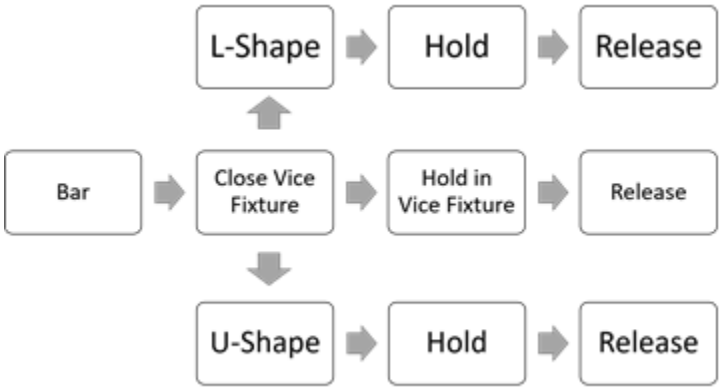

Figure 2. The initial bar undergoes 3 simple setups in the simulation: 1. clamp, hold, release. 2. clamp, hold, L-shape, hold, release. 3. clamp, hold, U-shape, hold, release.

The aluminum bar is held in position of the two vice plates for 2 x 10^{-10} seconds. The processing steps for the MD simulation after the bar is held in the vice fixture are as follows, and shown in Figure 2:

1. The vice plates are moved away at 10 m/s from the Al workpiece.
2. One fourth (top right section) of Al bar atoms are deleted to construct an L-shape. The fixed vice plates hold the leftover atoms (L-shape) for 2 x 10^{-10}s and then release at 10 m/s.
3. The center of the top half atoms with a width of 10 nm are deleted to construct a U-shape. The U-shape formed is subjected to the same processing as the L-shape in which the vice holds and releases the workpiece.

The simulations take a computation time of around 4 days on a 128-core machine for relaxation and 8 days for the fixture simulation. In view of this computational cost, we perform only a single simulation for each workpiece geometry in the present work.

For visualization and rendering of the figures, we use the free software tool OVITO [37]. The hydrostatic stress is calculated locally using the LAMMPS software. To this end, the forces acting on the atoms are evaluated to calculate the atomic virial, which – together with the local kinetic energy density – make up the local stress [38]. In the figures, stresses are averaged over a region of 4 nm.

4. RESULTS & DISCUSSION

After each of the processing steps was completed, the results of the atomic stresses were obtained. The stress distributions in the bar are shown after the vice was closed (Figure 3) and after the vice was held for 2 x 10^{-10} seconds (Figure 4). After the sample is fixed (Figure 3), a nearly symmetrical distribution of compressive stress builds up in the region compressed by the fixtures. The stress also reaches the upper part of the workpiece in an arch-bridge shape. The stress changes remarkably after holding for 2 x 10^{-10} seconds (Figure 4). The left-right symmetry is lost; this is due to the formation of plasticity, which occurs in the atomistic simulation in a strongly localized way, for instance at the upper edge of the left fixture. Since the generation of plasticity requires the nucleation of dislocations, and this is a stochastic process subject to local stress and temperature fluctuations, plasticity is not generated homogeneously in the workpiece. Figure 4 exemplifies the plasticity generated by displaying atomistically a stacking fault ribbon of a dislocation formed in Al; similar features can be observed at other spots on the workpiece. The bottom figure zooms into the rectangle area of the top figure, where the green line is a 1/6[112] dislocation and red atoms are stacking faults.

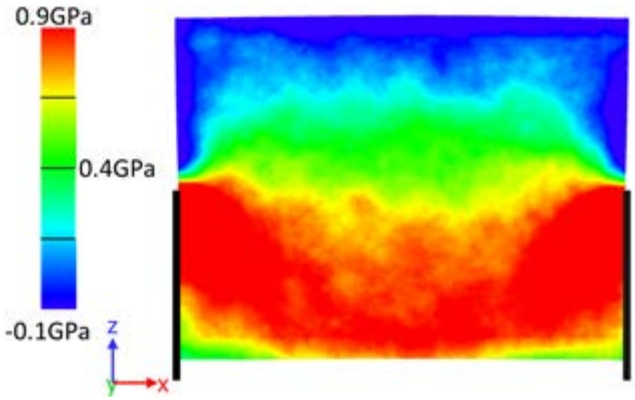

Figure 3. The stress distribution (in the frontal x-z plane) of the bar sample after each vice moved into the bar by 2 nm.

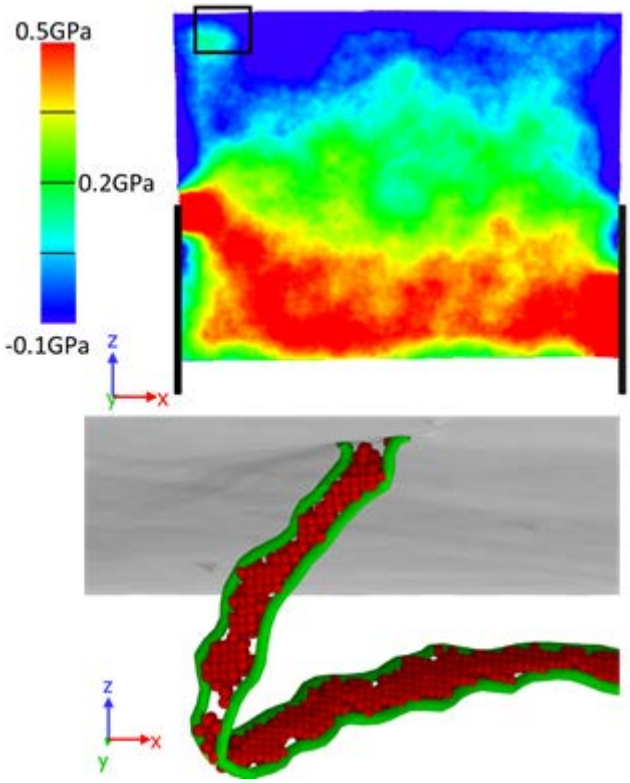

Figure 4. The stress distribution of the bar sample after being held in the vice for 2 x 10^{-10} second. The bottom image describes the dislocation found in the top left corner box.

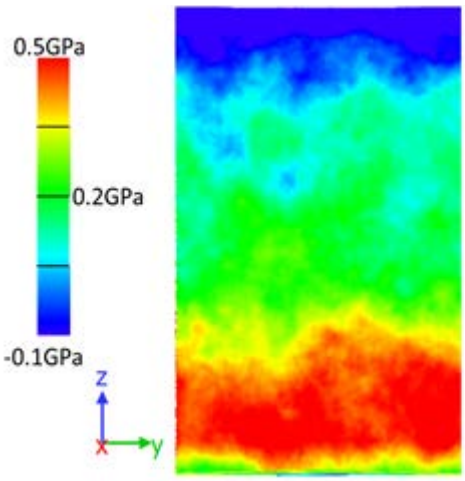

Figure 5. The stress distribution in the mid-plane cross section (y-z plane) after the bar sample was held in the vice for 2 x 10^{-10} second.

Figure 5 shows the stress distribution in the mid-plane of the bar sample, in between the vice fixtures. The stress is very homogeneous in the y direction. The lower half of the section is in compression while the upper half is in tension.

Figure 6 shows the stress distribution in the bar after being released from the fixture. The stress takes considerably smaller values than while being held in the fixtures; it takes values in the range of up to 100 MPa. The stress is dominantly compressive; stress maxima are concentrated on the left-hand side due to the generation of plasticity discussed above. The stress shown here is the residual stress as calculated in our atomistic simulation.

The resulting distortions are assembled in Figure 7, which provides the data in fractional changes which are useful to relate our results to actual measurements. The workpiece grew in height, while it narrowed in the length dimension. Note that the changes are not uniform. The height increase is concentrated on the left-hand side and the middle part, corresponding to the

plasticity generated there. Length changes are most pronounced at the bottom part, where the fixtures were applied.

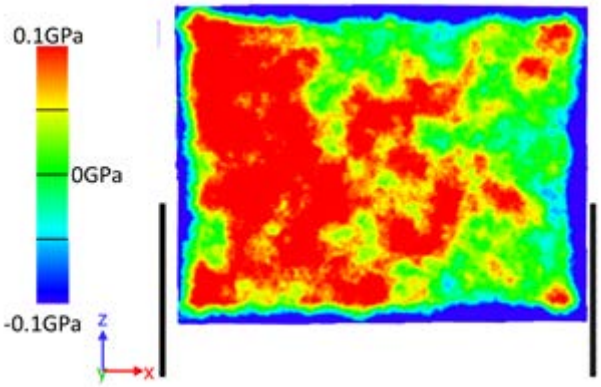

Figure 6. The stress distribution of the bar sample after being released from the vice fixture.

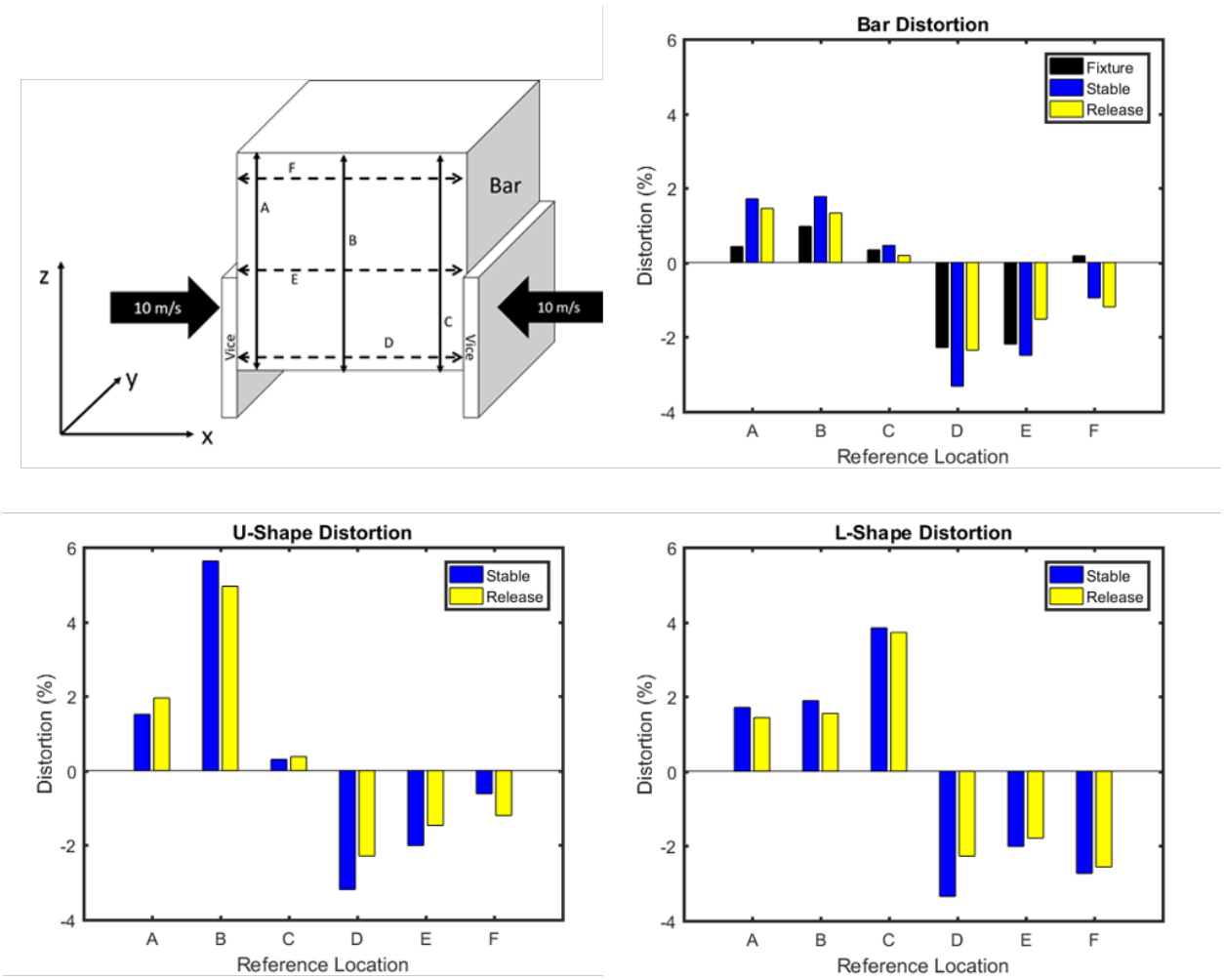

Figure 7. The distortion as percentages (%) for each sample (Bar, U-shape, and L-shape) and their respective locations (A, B, C, D, E, and F) are plotted.

The stress distribution in the U-shaped sample is shown in Figure 8 after holding the sample in the fixtures. Again, the stress is mainly concentrated between the fixtures, in the lower part of the workpiece, and the strong left-right asymmetry is caused by the nucleation of dislocations in the right-hand side, close to the fixtures. The corners of the U-shaped groove are under tensile stress. The height distortion, in particular along the line B (Figure 1), is now considerably larger than for the bar. The reason is that the lower part of the workpiece has

more freedom of being pushed up in the U groove than for a solid bar. Length changes are of a similar size, but somewhat smaller than for the bar shape.

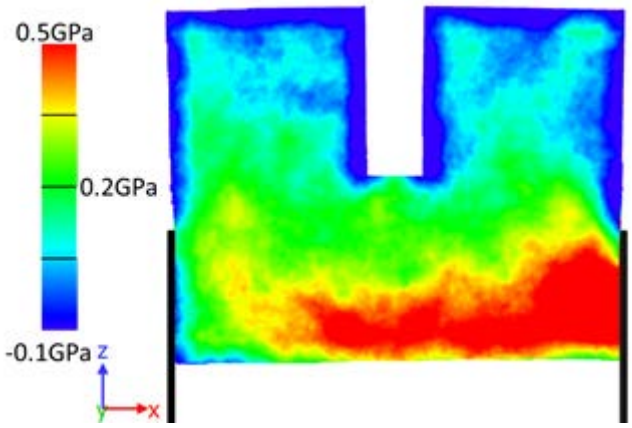

Figure 8. The stress distribution (in the frontal plane) of the U-shaped sample in the fixture after being held in the vice for 2 x 10^{-10} second.

After release of the fixtures, the stress in the U-shaped sample is very inhomogeneous as seen in Figure 9. In the left-hand side corner of the U groove, tensile stress has been kept and expanded, while compressive stress is generated in the right-hand side part. This example demonstrates the occurrence of strongly inhomogeneous residual stress distributions caused by the local generation of plasticity. The strong distortions that were established during the holding phase survive after removing the fixtures, see Figure 7.

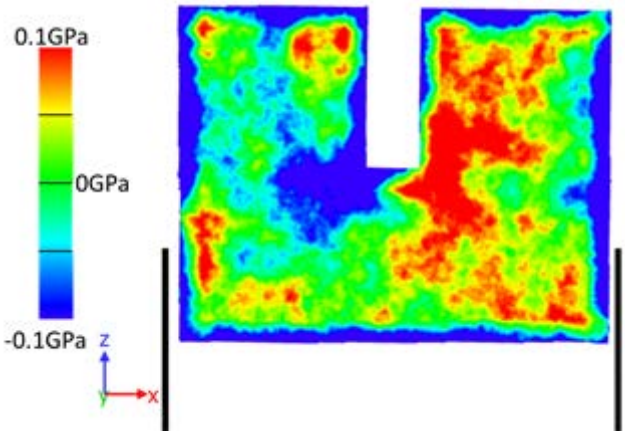

Figure 9. The stress distribution (in the frontal plane) of the U-shape sample after it was released from the vice fixture.

Furthermore, Figure 10 shows the stress distribution in the L-shaped workpiece after holding it in the vice. Compressive stress is concentrated in the right-hand side; the material above the fixtures on the left-hand side helps alleviate the pressure in the left-hand side. Height distortions are now particularly large in the middle of the workpiece, along line B (Figure 1), see Figure 7.

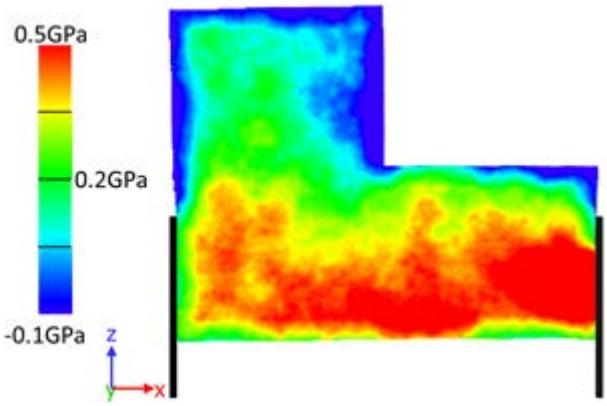

Figure 10. The stress distribution (in the frontal plane) of the L-shaped sample in the fixture after being held in the vice for 2 x 10^{-10} second.

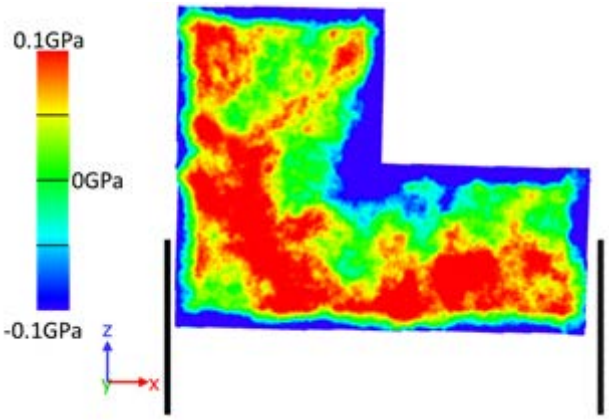

Figure 11. The stress distribution of the L-shape sample after it was released from the vice fixture.

After the L-shape is released from the fixture, the entire sample is under compressive stresses, as seen in Figure 11. Note that the L-shaped sample is rotated during releasing due to the asymmetric shape.

These results provide information about the critical locations in which the workpiece may be affected by the fixture contact. The results show that the vice fixture deforms the single grain pure Al sample both elastically and plastically to cause overall part distortion shown in the bottom edge of the release figure of each case being deformed from its original position. We note that we performed only a single simulation for each workpiece. While, due to thermal fluctuations, the exact position of the plastic material failure is subject to statistics, it is not the aim of the present work to calculate averages over these thermal fluctuations, but rather to help understand where these fluctuations occur and how they contribute to distortions. The analysis of statistical fluctuations will be more important in future work, where crystal defects in the workpiece will be considered.

Overall, the results give insight to how nano-manufacturing components deform due to fixture parameters while in the vice. At the nano scale, holding a part in a fixture with a 10 m/s closing velocity experiences distortions. The effect of fixtures and work holding devices at a smaller level could have potentially larger effects than that of the macro scale. In addition, understanding how a workpiece deforms while in the fixture suggests further research at both the macro and nano scale to understand machining distortions due to fixture stresses. More work is needed to analyze the effects of clamping in relation to manufacturing for both macro and nano processes.

5. CONCLUSION

In conclusion, the overall purpose of this paper is to investigate the relation of macro and nano machining by understanding fixtures and work holding devices. Through this work, simulations of nano scale geometries revealed machining distortions and critical stress concentrations directly related to the fixture.

A major result of this work is that the residual stresses formed could be related to the local generation of plasticity. In addition, it was shown that the local plasticity leads to strongly inhomogeneous residual stress distributions, which do not follow the symmetries of the workpiece.

Future work is needed to further investigate the applicability of using nano-machining simulations to understand macro machining. An important step that needs to be taken is the inclusion of pre-existing defects in the workpiece, in particular grain boundaries and dislocations; also the effect of rough surfaces needs to be investigated. For such future

investigations, the present study will serve as a reference, as it details the effects in an ideal – i.e., single-crystalline and defect-free workpiece. More research towards fixture related distortion and deformation is needed to fully digest the relation between the two machining scales. All in all, the results from the simulations provide an insight to the behavior of workpieces while in a fixture for manufacturing applications. The results showed an importance of the clamping forces for nano-manufacturing.

6. ACKNOWLEDGMENTS

Simulations were performed at the High Performance Cluster Elwetritsch (RHRK, TU Kaiserslautern, Germany). Collaboration under the International Research Training Group (IRTG) 2057 received financial support from the Deutsche Forschungsgemeinschaft.

Author contributions

Z. Zhang performed the simulations and analysis. D. R. Garcia wrote the paper. All authors designed and discussed the work. Prof. Linke and Prof. Urbassek supervised this work.

References

1. J. Chae, S. S. Park, and T. Freiheit, “Investigation of micro-cutting operations,” *Int. J. Mach. Tools Manuf.*, vol. 46, no. 3–4, pp. 313–332, Mar. 2006.

2. Chantzis, D., Van-der-Veen, S., Zettler, J., Sim, W.M., An Industrial Workflow to Minimise Part Distortion for Machining of Large Monolithic Components in Aerospace Industry, Procedia CIRP, Volume 8, p. 281-286, ISSN 2212-827, 2013.

3. Shigeo Sato, Kazuaki Wagatsuma, Shigeru Suzuki, Masayoshi Kumagai, Muneyuki Imafuku, Hitoshi Tashiro, Kentaro Kajiwara, Takahiasa Shobu, Relationship between dislocations and residual stresses in cold-drawn pearlitic steel analyzed by energy-dispersive X-ray diffraction, Materials Characterization, Volume 83, September 2013, Pages 152-160, ISSN 1044-5803, http://dx.doi.org/10.1016/j.matchar.2013.06.017

4. Schajer, G. S., Ruud, C. O., Overview of Residual Stresses and Their Measurement, Practical Residual Stress Measurement Methods, John Wiley & Sons, Ltd, p. 1–27, 2013.

5. Li, J., Wang, S., Distortion caused by residual stresses in machining aeronautical aluminum alloy parts: recent advances. The International Journal of Advanced Manufacturing Technology, 1–16. article. http://doi.org/10.1007/s00170-016-9066-6, 2016.

6. Zhang, Z., Li, L., Yang, Y., He, N., Zhao, W., Machining distortion minimization for the manufacturing of aeronautical structure, Int. J. Adv. Manuf. Technol., vol. 73, no. 9, p. 1765–1773, 2014.

7. Schulze, V., Arrazola, P., Zanger, F., Osterried, J., Simulation of distortion due to machining of thin-walled components, Procedia CIRP, vol. 8, p. 45–50, 2013.

8. Guo, H., Zuo, D. W., Wu, H. B., Xu, F., Tong, G. Q., Prediction on milling distortion for aero-multi-frame parts, Mater. Sci. Eng. A, vol. 499, no. 1–2, p. 230–233, 2009.

9. Huang, X., Sun, J., Li, J., Finite element simulation and experimental investigation on the residual stress- related monolithic component deformation, International Journal of Advanced Manufacturing Technology, Volume 77, Issue 5, pp 1035–1041 doi:10.1007/s00170-014- 6533-9, 2015.

10. D'Alvise, L., Chantzis, D., Schoinochoritis, B., Salonitis, K., Modelling of Part Distortion Due to Residual Stresses Relaxation: An aeronautical Case Study, Procedia CIRP, vol. 31, p. 447–452, 2015.

11. Zhang, L., Feng, X., Li, Z., Liu, C., FEM simulation and experimental study on the quenching residual stress of aluminum alloy 2024, Proc. Inst. Mech. Eng. Part B J. Eng. Manuf., May 2013.

12. Loehe, J., Zaeh, M. F., Roesch, O., In-process deformation measurement of thin-walled workpieces, Procedia CIRP, vol. 1, no. 1, p. 546–551, 2012.

13. Brinksmeier, E., Lübben T., Fritsching U., Cui C., Rentsch R., Sölter, J., Distortion minimization of disks for gear manufacture, Int. J. Mach. Tools Manuf., vol. 51, no. 4, p. 331–338, 2011.

14. D. Dornfeld, S. Min, and Y. Takeuchi, "Recent Advances in Mechanical Micromachining," *CIRP Ann. - Manuf. Technol.*, vol. 55, no. 2, pp. 745–768, 2006.

15. D. Cui, L. Zhang, K. Mylvaganam, W. Liu, and W. Xu, "Nano-milling on monocrystalline copper: A molecular dynamics simulation," *Mach. Sci. Technol.*, vol. 21, no. 1, pp. 67–85, 2017.

16. U. Kunze, "Invited Review Nanoscale devices fabricated by dynamic ploughing with an atomic force microscope," *Superlattices Microstruct.*, vol. 31, no. 1, pp. 3–17, 2002.

17. Z. PZ, C. Qiu, F. FZ, Y. DD, and S. XC, "Molecular dynamics simulations of nanometric cutting mechanisms of amorphous alloy," *Appl. Surf. Sci.*, vol. 317, pp. 432–442, 2014.

18. L. Zhang and H. Tanaka, "Atomic scale deformation in silicon monocrystals induced by two-body and three-body contact sliding," *Tribol. Int.*, vol. 31, no. 8, pp. 425–433, 1998.

19. N. Tansel, T. T. Arkan, W. Y. Bao, N. Mahendrakar, B. Shisler, D. Smith, and M. McCool, "Tool wear estimation in micro-machining. Part I: Tool usage-cutting force relationship," *Int. J. Mach. Tools Manuf.*, vol. 40, no. 4, pp. 599–608, 2000.

20. J. Fleischer and J. Kotschenreuther, "The manufacturing of micro molds by conventional and energy-assisted processes," *Int. J. Adv. Manuf. Technol.*, vol. 33, no. 1–2, pp. 75–85, 2007.

21. Hesse, S., Krahn, H., Eh, D.: Betriebsmittel Vorrichtung. Carl Hanser Verlag München, 2012

22. H.-C. Möhring and P. Wiederkehr, "Intelligent Fixtures for High Performance Machining," *Procedia CIRP*, vol. 46, pp. 383–390, 2016.

23. W. Chen, L. Ni, and J. Xue, "Deformation control through fixture layout design and clamping force optimization," *Int. J. Adv. Manuf. Technol.*, vol. 38, no. 9, p. 860, 2007.

24. Asante, J.N. Int J Adv Manuf Technol (2008) 39: 578. doi:10.1007/s00170-007-1187-5

25. Krar, Stephen F., Arthur Gill, and Peter Smid. Technology of Machine Tools. New York: McGraw Hill, 2011. Print.

26. S. Pehlivan and J. D. Summers, “A review of computer-aided fixture design with respect to information support requirements,” *Int. J. Prod. Res.*, vol. 46, no. 4, pp. 929–947, Feb. 2008.

27. B. Li and S. N. Melkote, “Fixture Clamping Force Optimisation and its Impact on Workpiece Location Accuracy,” *Int. J. Adv. Manuf. Technol.*, vol. 17, no. 2, pp. 104–113, 2001.

28. Boyle, Y. M. Rong, and D. C. Brown, “A review and analysis of current computer-aided fixture design approaches,” *Robot. Comput. Integr. Manuf.*, vol. 27, no. 1, pp. 1–12, Feb. 2011.

29. Z. M. Bi and W. J. Zhang, “Flexible fixture design and automation: Review, issues and future directions,” *Int. J. Prod. Res.*, vol. 39, no. 13, pp. 2867–2894, Jan. 2001.

30. B. Tadic, D. Vukelic, D. Miljanic, B. Bogdanovic, I. Macuzic, I. Budak, and P. Todorovic, "Model testing of fixture–workpiece interface compliance in dynamic conditions," *J. Manuf. Syst.*, vol. 33, no. 1, pp. 76–83, Jan. 2014.

31. T. Papastathis, O. Bakker, S. Ratchev, and A. Popov, "Design Methodology for Mechatronic Active Fixtures with Movable Clamps," *Procedia CIRP*, vol. 3, pp. 323–328, 2012.

32. S. Plimpton, Fast Parallel Algorithms for Short-Range Molecular Dynamics, J Comp Phys, 117, 1-19 (1995). http://lammps.sandia.gov.

33. Daw, M. S.; Baskes, M. I. Semiempirical, Quantum Mechanical Calculation of Hydrogen Embrittlement in Metals. Physical Review Letters, 1983, 50, 1285-1288

34. Mendelev, M. I.; Kramer, M. J.; Becker, C. A.; Asta, M. Analysis of semi-empirical interatomic potentials appropriate for simulation of crystalline and liquid Al and Cu. Philosophical Magazine, 2008, 88, 1723-1750.

35. Iyad Alabd Alhafez, Yu Gao and Herbert M. Urbassek,Nanocutting: A Comparative Molecular-Dynamics Study of Fcc, Bcc, and Hcp Metals,Current Nanoscience, volume 13, issue 1, pages 40-47, year 2017, issn 1573-4137/1875-6786, doi 10.2174/1573413712666160530123834

36. Ruestes, C. J.; Bringa, E. M.; Gao, Y.; Urbassek, H. M. "Molecular dynamics modeling of nanoindentation", in Applied nanoindentation in advanced materials, edited by A. Tiwari and S. Natarajan (Wiley, Chichester, UK, 2017) Chap. 14, pp. 313-345.

37. Stukowski A., Visualization and analysis of atomistic simulation data with OVITO – the Open Visualization Tool. Model. Simul. Mater. Sci. Eng. 18 (2010) 015012. http://www.ovito.org/

38. Frenkel, D.; Smit, B. Understanding molecular simulations: From algorithms to applications. Academic, 1996.